

Convergence conditions for iterative methods seeking multi-component solitary waves with prescribed quadratic conserved quantities

T.I. Lakoba*

Department of Mathematics and Statistics, 16 Colchester Ave.,
University of Vermont, Burlington, VT 05401, USA

December 2, 2010

Abstract

We obtain linearized (i.e., non-global) convergence conditions for iterative methods that seek solitary waves with prescribed values of quadratic conserved quantities of multi-component Hamiltonian nonlinear wave equations. These conditions extend the ones found for single-component solitary waves in a recent publication by J. Yang and the present author. We also show that, and why, these convergence conditions coincide with dynamical stability conditions for ground-state solitary waves.

Notably, our analysis applies regardless of whether the number of quadratic conserved quantities, s , equals or is less than the number of equations, S . To illustrate the situation when $s < S$, we use one of our iterative methods to find ground-state solitary waves in spin-1 Bose–Einstein condensates in a magnetic field ($s = 2$, $S = 3$).

Keywords: Coupled nonlinear wave equations, Solitary waves, Iterative methods, spinor Bose–Einstein condensates.

*lakobati@cems.uvm.edu, 1 (802) 656-2610

1 Introduction and background

Solitary wave solutions of most nonlinear wave equations can be found only numerically. Recently, J. Yang and the present author obtained [22] conditions under which an iterative numerical method can converge to stationary solitary waves of single-component Hamiltonian nonlinear wave equations. When this method, in what follows referred to as the imaginary-time evolution method (ITEM), converges, it provides one with a numerical approximation of a solitary waves with a prescribed value of a quadratic conserved quantity usually referred to either as *power* or the number of particles. However, many phenomena are described not by a single equation but by systems of coupled equations. Therefore, it is of interest to obtain conditions under which a multi-component counterpart of the ITEM would be guaranteed to converge to a multi-component solitary wave. We obtain such a condition in this work. Moreover, generalizing an observation made in [22], we show that the multi-component ITEM converges only to those ground states of nonlinear wave equations which are dynamically stable, and explain why this is the case.

For the single-equation case considered in Ref. [22], the power of a solitary wave is

$$P = \int u^2(\mathbf{x}) d\mathbf{x}, \quad (1.1)$$

where u is the real-valued field of the solitary wave and \mathbf{x} is the spatial coordinate. (Here and below, if the limits of the integration are not indicated, the integration is assumed to be over the entire spatial domain.) For example, if the time-dependent wave $U(\mathbf{x}, t)$ satisfies a Nonlinear Schrödinger-type (NLS-type) equation

$$iU_t + \nabla^2 U + G(|U|^2, \mathbf{x})U = 0, \quad U(|\mathbf{x}| \rightarrow \infty) \rightarrow 0, \quad (1.2)$$

where ∇^2 is the Laplacian, then upon the substitution $U(\mathbf{x}, t) = e^{i\mu t}u(\mathbf{x})$, where u is real, Eq. (1.2) reduces to

$$L^{(00)}u - \mu u \equiv L^{(0)}u = 0, \quad (1.3a)$$

where

$$L^{(00)}u \equiv \nabla^2 u + G(u^2, \mathbf{x})u. \quad (1.3b)$$

The parameter μ is referred to as the propagation constant of the solitary wave. A straightforward calculation shows that the power $P = \int u^2 d\mathbf{x} = \int |U|^2 d\mathbf{x}$ is conserved by the evolution equation (1.2). Thus, u can be parametrized either by P or by μ , so that one can write $P \equiv P(\mu)$.

The method analyzed in [22] finds the solution u with a prescribed value of P by iterations:

$$\mu_n = \frac{\langle N^{-1}u_n, L^{(00)}u_n \rangle}{\langle N^{-1}u_n, u_n \rangle}, \quad (1.4a)$$

$$\hat{u}_{n+1} - u_n = N^{-1} \left(L^{(00)}u_n - \mu_n u_n \right) \Delta\tau, \quad (1.4b)$$

$$u_{n+1} = \hat{u}_{n+1} \sqrt{\frac{P}{\langle \hat{u}_{n+1}, \hat{u}_{n+1} \rangle}}. \quad (1.4c)$$

where $\Delta\tau > 0$ is an auxiliary parameter, and a positive definite operator N can be conveniently chosen in the form mimicking the linear constant-coefficient part of $L^{(0)}$ in (1.3a):

$$N = c - \nabla^2, \quad c > 0. \quad (1.5)$$

The purposes of $\Delta\tau$ and N^{-1} in (1.4b) will be clarified shortly. The inner product is defined as

$$\langle f(\mathbf{x}), g(\mathbf{x}) \rangle \equiv \int (f(\mathbf{x}))^T g(\mathbf{x}) d\mathbf{x}. \quad (1.6)$$

Methods similar to (1.4) had also been considered for finding solitary waves in the past (see, e.g., [1, 2, 6, 7, 18]). However, it was in [22] where the convergence conditions of the specific version, (1.4), of the ITEM were found in terms of the properties of the linearized operator of Eq. (1.3a). Namely, Eqs. (1.4) are linearized by a substitution

$$u_n = u + \tilde{u}_n, \quad |\tilde{u}_n| \ll u, \quad (1.7)$$

which results in [22]

$$\tilde{u}_{n+1} - \tilde{u}_n = N^{-1} \mathcal{L} \tilde{u}_n \Delta\tau, \quad \mathcal{L} \tilde{u}_n \equiv L \tilde{u}_n - \frac{\langle N^{-1} u, L \tilde{u}_n \rangle}{\langle N^{-1} u, u \rangle} u. \quad (1.8)$$

Here L is the linearized operator of $L^{(0)}$ in Eq. (1.3a). For example, for $L^{(0)}$ given by (1.3b),

$$L = \nabla^2 - \mu + G(u^2, \mathbf{x}) + 2u^2 G_{u^2}(u^2, \mathbf{x}). \quad (1.9)$$

The ITEM (1.4) converges if the eigenvalues of the right-hand side of its linearization (1.8) are located between -2 and 0 . The first of these conditions implies that

$$\Delta\tau < -2/\Lambda_{\min}, \quad (1.10)$$

where Λ_{\min} is the most negative eigenvalue of $N^{-1} \mathcal{L}$. (In practice, the maximum $\Delta\tau_{\max}$ can be easily found by just a few trials, and then the value $\Delta\tau$ leading to an optimal convergence rate is usually somewhat smaller than $\Delta\tau_{\max}$; see Fig. 3 and Eq. (47) in [22].) The second condition can be shown [22] to be related to the properties of the original equation (1.3a) and its linearized operator L as follows¹. First, let us denote

$$p(L) \equiv \text{the number of positive eigenvalues of } L \text{ counting their multiplicity} \quad (1.11)$$

(and similarly for any other operator or matrix). Next, assume that we are considering the generic case whereby the null space of L does not contain any functions other than those of

¹In the language of Linear Algebra, \mathcal{L} differs from L by a rank-one correction (i.e., the last term in (1.8)), and the relation between the eigenvalues of two such matrices can be found, e.g., in [19], p. 230.

the modes $\partial u/\partial x^{(k)}$ which are associated with translational invariance of the solitary wave along $x^{(k)}$. Then, under condition (1.10), the ITEM (1.4) converges provided that either

$$p(L) = 0 \quad \text{and} \quad \partial P/\partial \mu \neq 0, \quad (1.12a)$$

or

$$p(L) = 1 \quad \text{and} \quad \partial P/\partial \mu > 0. \quad (1.12b)$$

In all the other cases algorithm (1.4) diverges². Remarkably, as pointed out in [22], these convergence conditions are the same as the Vakhitov–Kolokolov stability conditions of nodeless solitary waves in the NLS-type evolution equation (1.2) [20, 12]. In other words, the ITEM (1.4) converges only to those nodeless solitary waves of (1.2) that are dynamically linearly stable. (Let us note, in passing, that iterative methods that are guaranteed to converge to *any* solitary wave, stable or unstable, were first proposed in [7] and later developed in [21].)

The purpose of using operator N^{-1} in (1.4b) is to considerably reduce the magnitude of the most negative eigenvalue of operator $N^{-1}\mathcal{L}$ compared to that of L [7, 22, 21]. This is analogous to preconditioning a poorly conditioned matrix A when solving a linear equation $A\mathbf{y} = \mathbf{b}$ by an iterative method; this can considerably improve the convergence rate of the iterations (see, e.g., [19], Lecture 40). In regards to implementing N , note that it is a differential operator with constant coefficients and hence has a simple representation in the Fourier space. Therefore, $N^{-1}L^{(00)}u_n$ and $N^{-1}u_n$ are easily computed using the direct and inverse Fast Fourier Transforms, which are available as built-in commands in all major computing software.

Note that the propagation constant μ in the ITEM (1.4) is not prescribed but computed iteratively. Numerical methods for finding solutions of Eq. (1.3) with a specified value of μ rather than with a specified value of power (1.1) have also been considered in quite a few studies (see, e.g., references in [15]), and we will not consider them in this work.

In this paper, we derive convergence conditions of a generalization of the ITEM (1.4) for multi-component solitary waves. Such a generalization was proposed in [15] (but see also Section 4.3 in [21]), and its algorithm is presented in Section 2. Note that in [15], we also proposed another method that finds solitary waves with the same conserved quantities as the ITEM but converges faster; moreover, it converges *much* faster than the ITEM when the latter converges slowly. This method is a modified form of the well-known Conjugate Gradient method (CGM; see, e.g., [19], Lecture 38), and its algorithm is given in Appendix A for the reader's convenience. In [15] we showed that this modified CGM has the same convergence conditions as the ITEM. Therefore, these convergence conditions, which generalize conditions (1.12), apply to both the ITEM and modified CGM. The derivation of these

²In [22] it was also required that for $p(L) = 1$, the eigenfunction of $N^{-1}L$ corresponding to the positive eigenvalue be not orthogonal to u . However, one can show, similarly to how we will do it in Section 3, that this special case actually falls under case (1.12b).

conditions is the main result of this paper and is presented in Section 3. This derivation follows the lines of Ref. [17], where it was used to establish *stability* conditions for a certain class of multi-component solitary waves. In fact, our convergence conditions of the ITEM and modified CGM turn out to be the same as the stability conditions derived in [17]. This relation between the two sets of conditions generalizes a similar fact pointed out in [22] for single-component equations, and in Section 4 we explain under what circumstances such a coincidence of the convergence and stability conditions occurs. In Section 5 we demonstrate the validity of the convergence conditions derived in Section 3 for a system describing the ground-state solution of a multi-component Bose–Einstein condensate (BEC). Other examples involving the multi-component ITEM and CGM can be found in Ref. [15]; see also Example 6 in [21] for a related method. In Section 6 we summarize the results of this work. In Appendix B we present the forms of the ITEM and CGM applicable to complex-valued equations. In Appendix C we provide a geometrical argument that facilitates intuitive interpretation of the convergence conditions derived in Section 3 for the special case where the solitary wave has two quadratic conserved quantities.

The example of a multi-component BEC considered in Section 5 has a notable feature that its number of quadratic conserved quantities is less than the number of the solitary wave’s components. Modifications of the ITEM for that type of problems were earlier proposed in [4, 3]. Our modification of the ITEM is different from those and is both conceptually and technically simpler. We will discuss this further in Sections 2 and 5.

2 ITEM algorithm for multi-component solitary waves

Let us begin with a relatively simple example that will motivate introduction of some new notations. A more complicated example of spin-1 BEC is considered in Section 5. The following system describes pulse evolution in a two-core nonlinear directional fiber coupler where each core supports two orthogonal polarizations of light [13]:

$$\begin{aligned}
iU_t^{(1)} + U_{xx}^{(1)} + \left(|U^{(1)}|^2 + \kappa|U^{(2)}|^2\right)U^{(1)} + U^{(3)} &= 0 \\
iU_t^{(2)} + U_{xx}^{(2)} + \left(|U^{(2)}|^2 + \kappa|U^{(1)}|^2\right)U^{(2)} + U^{(4)} &= 0 \\
iU_t^{(3)} + U_{xx}^{(3)} + \left(|U^{(3)}|^2 + \kappa|U^{(4)}|^2\right)U^{(3)} + U^{(1)} &= 0 \\
iU_t^{(4)} + U_{xx}^{(4)} + \left(|U^{(4)}|^2 + \kappa|U^{(3)}|^2\right)U^{(4)} + U^{(2)} &= 0
\end{aligned} \tag{2.1}$$

Here $(U^{(1)}, U^{(2)})$ and $(U^{(3)}, U^{(4)})$ are the pairs of orthogonal polarizations in the two cores. The quadratic quantities conserved by these equations and generalizing (1.1) are:

$$\vec{Q} = \begin{pmatrix} P^{(1)} + P^{(3)} \\ P^{(2)} + P^{(4)} \end{pmatrix} \equiv \begin{pmatrix} 1 & 0 & 1 & 0 \\ 0 & 1 & 0 & 1 \end{pmatrix} \begin{pmatrix} P^{(1)} \\ P^{(2)} \\ P^{(3)} \\ P^{(4)} \end{pmatrix}, \tag{2.2}$$

where $P^{(k)} = \langle (U^{(k)})^*, U^{(k)} \rangle$. Upon the substitution

$$\begin{pmatrix} U^{(1)}(x, t) \\ U^{(2)}(x, t) \\ U^{(3)}(x, t) \\ U^{(4)}(x, t) \end{pmatrix} = \begin{pmatrix} u^{(1)}(x) & 0 \\ 0 & u^{(2)}(x) \\ u^{(3)}(x) & 0 \\ 0 & u^{(4)}(x) \end{pmatrix} \begin{pmatrix} e^{i\mu^{(1)}t} \\ e^{i\mu^{(2)}t} \end{pmatrix}, \quad (2.3)$$

where $u^{(k)}$ can (for the purpose of this example) be chosen to be real-valued, system (2.1) reduces to:

$$\begin{pmatrix} u_{xx}^{(1)} + ((u^{(1)})^2 + \kappa(u^{(2)})^2) u^{(1)} + u^{(3)} \\ u_{xx}^{(2)} + ((u^{(2)})^2 + \kappa(u^{(1)})^2) u^{(2)} + u^{(4)} \\ u_{xx}^{(3)} + ((u^{(3)})^2 + \kappa(u^{(4)})^2) u^{(3)} + u^{(1)} \\ u_{xx}^{(4)} + ((u^{(4)})^2 + \kappa(u^{(3)})^2) u^{(4)} + u^{(2)} \end{pmatrix} - \begin{pmatrix} u^{(1)} & 0 \\ 0 & u^{(2)} \\ u^{(3)} & 0 \\ 0 & u^{(4)} \end{pmatrix} \vec{\mu} = \begin{pmatrix} 0 \\ 0 \\ 0 \\ 0 \end{pmatrix}, \quad (2.4)$$

where $\vec{\mu} = (\mu^{(1)}, \mu^{(2)})^T$. Then the powers of the individual components are

$$P^{(k)} = \langle u^{(k)}, u^{(k)} \rangle. \quad (2.5)$$

We now generalize this example to an S -component system possessing an s -component vector of conserved quantities \vec{Q} , so that the k th component of \vec{Q} is:

$$Q^{(k)} = \sum_{l=1}^S q^{(kl)} P^{(l)}, \quad k = 1, \dots, s \leq S, \quad l = 1, \dots, S, \quad (2.6)$$

where the solitary wave is $\mathbf{u} = (u^{(1)}, \dots, u^{(S)})^T$. As illustrated in the above example with $S = 4$ and $s = 2$, the number of conserved quantities can be less than the number of the components of the solitary wave: $s \leq S$. Other examples where the situation $s < S$ takes place include: the system of three waves interacting via quadratic nonlinearity [10, 5]; any system of coupled carrier-wave (also known as long-wave, or Korteweg–de Vries-type (KdV-type)) equations, as we will explain at the end of Section 4; and a system of NLS-type equations coupled coherently via phase-sensitive *nonlinear* terms (as opposed to linear ones as in (2.1)). Equations of spinor BEC, considered in Section 5, are a special case of the latter example. To emphasize the possibility of having $s < S$, we use a different vector notation for \vec{Q} than for \mathbf{u} . Now, the matrix $(q^{(kl)})$ in (2.6) is assumed to be in reduced echelon form (REF; see any textbook on undergraduate Linear Algebra) and, in addition, its columns are arranged so that

$$q^{(kl)} = \begin{cases} 0, & l < k \\ 1, & l = k. \end{cases} \quad (2.7)$$

In (2.2), matrix $(q^{(kl)})$ is the 2×4 matrix, which is in REF. The above assumptions about matrix $q^{(kl)}$ are not at all restrictive, as we demonstrate in Section 5, where $q^{(kl)}$ is initially not in REF.

The multi-component generalization of Eqs. (1.3a) and (1.4a) is

$$\mathbf{L}^{(0)}\mathbf{u} \equiv \mathbf{L}^{(00)}\mathbf{u} - \mathcal{U} \langle \mathbf{N}^{-1}\mathcal{U}, \mathcal{U} \rangle^{-1} \langle \mathbf{N}^{-1}\mathcal{U}, \mathbf{L}^{(00)}\mathbf{u} \rangle = \mathbf{0}, \quad (2.8a)$$

$$\mathcal{U} \equiv \frac{\delta \vec{Q}}{\delta \mathbf{u}}. \quad (2.8b)$$

For example, in (2.4), $\mathbf{L}^{(00)}\mathbf{u}$ is the first term (the 4×1 vector), and \mathcal{U} is the first factor of the second term (the 4×2 matrix) on the left-hand side. Thus, by analogy with (2.4),

$$\langle \mathbf{N}^{-1}\mathcal{U}, \mathcal{U} \rangle^{-1} \langle \mathbf{N}^{-1}\mathcal{U}, \mathbf{L}^{(00)}\mathbf{u} \rangle = \vec{\mu}. \quad (2.8c)$$

The $S \times S$ matrix \mathbf{N} is a self-adjoint positive definite operator. For optimal preconditioning, its differential part should mimic the highest derivative in the linear part of $\mathbf{L}^{(00)}$. For example, for the $\mathbf{L}^{(00)}$ in (2.4), \mathbf{N} can be chosen as a diagonal matrix with its diagonal entries of the form (1.5).

The multi-component version of the ITEM (1.4) is:

$$\hat{\mathbf{u}}_{n+1} - \mathbf{u}_n = \mathbf{N}^{-1} \left(\mathbf{L}^{(00)}\mathbf{u}_n - \mathcal{U}_n \langle \mathbf{N}^{-1}\mathcal{U}_n, \mathcal{U}_n \rangle^{-1} \langle \mathbf{N}^{-1}\mathcal{U}_n, \mathbf{L}^{(00)}\mathbf{u}_n \rangle \right) \Delta\tau, \quad (2.9a)$$

$$u_{n+1}^{(k)} = \hat{u}_{n+1}^{(k)} \sqrt{\frac{Q^{(k)} - \sum_{l=k+1}^S q^{(kl)} \hat{P}_{n+1}^{(l)}}{\hat{P}_{n+1}^{(k)}}}, \quad k = 1, \dots, s \leq S, \quad (2.9b)$$

$$u_{n+1}^{(k)} = \hat{u}_{n+1}^{(k)}, \quad k = s+1, \dots, S \quad (\text{if } s < S), \quad (2.9c)$$

where

$$\hat{P}_{n+1}^{(k)} \equiv \langle \hat{u}_{n+1}^{(k)}, \hat{u}_{n+1}^{(k)} \rangle, \quad k = 1, \dots, S.$$

Note that, by (2.7), the numerator of the fraction under the square root equals $P^{(k)}$. Let us emphasize that if $s < S$, then (2.9b) specifies only that the s components of \vec{Q} have their prescribed values but does not impose any other conditions on the powers, $P^{(k)}$, of the *individual* components of the solitary wave. Moreover, in that case the remaining $(S - s)$ components should *not* be normalized. Some issues of implementation of (2.9) are discussed in Section 5.

Three remarks about method (2.9) are in order before we proceed. First, we discuss its relation to similar methods proposed in the literature. The method proposed in [4] is conceptually equivalent to our Eq. (2.9a). As we point out after Eq. (2.11) below, step (2.9b) does not affect the convergence of the method. Rather, it merely ensures that the conserved quantities \vec{Q} keep their prescribed values at every iteration *exactly* instead of in the linear approximation, as Eq. (2.9a) alone (and hence the method of [4]) would do. In [3, 16] the authors proposed an alternative method that is similar to: Eq. (2.9a) *without the* $\vec{\mu}$ -*term* (see (2.8c)) plus the normalization (2.9b) plus *an additional* “fictitious” normalization of the remaining $(S - s)$ components of the solution (instead of our step (2.9c)). That method enforces \vec{Q} to take on their prescribed values exactly, and therefore is conceptually

equivalent to our method (2.9). However, we believe that our method is simpler than that of [3, 16] because: (i) It does not require the calculation of the fictitious normalization of the components $u^{(k)}$, $k = s + 1, \dots, S$; and (ii) because its form does not become any more complex as the number $(S - s)$ of such components increases, whereas the fictitious normalization (of a rather complex form) was worked out in [3] only for the case $S - s = 1$.

Second, as we noted in Section 1, in [15] we proposed a modified CGM that converges under the same conditions that we will establish for the ITEM (2.9), but faster. Moreover, it converges *much* faster when the ITEM converges slowly. Its algorithm, however, is somewhat less transparent than (2.9), and therefore we state it in Appendix A. Let us reiterate: The convergence analysis that we will present in Section 3 applies both to the ITEM and the modified CGM. We advocate using the latter method when the slow convergence of the ITEM justifies spending a little extra effort on programming the algorithm of the CGM.

Third, the ITEM (2.9), as well as the CGM in Appendix A, are stated for the case where each component of \mathbf{u} is a real-valued function. Clearly, any complex variable can be split into two real-valued components (real and imaginary parts), and so algorithms (2.9) and (A.1) can be applied to complex-valued equations in that manner. However, those algorithms can also be applied to complex equations *directly* (i.e., without splitting them into real and imaginary parts); the corresponding modified forms of (2.9) and (A.1) are listed in Appendix B.

We now return to the convergence analysis of the ITEM (2.9). As in the single-component case, we perform it using linearization analogous to (1.7). A tedious but straightforward calculation shows that the linearized operator of the right-hand side of Eq. (2.9a) is:

$$\mathbf{N}^{-1}\mathcal{L}\tilde{\mathbf{u}}_n \equiv \mathbf{N}^{-1}(\mathbf{L}\tilde{\mathbf{u}}_n - \mathcal{U}\langle\mathbf{N}^{-1}\mathcal{U}, \mathcal{U}\rangle^{-1}\langle\mathbf{N}^{-1}\mathcal{U}, \mathbf{L}\tilde{\mathbf{u}}_n\rangle). \quad (2.10)$$

Here \mathbf{L} is the linearized operator of $\mathbf{L}^{(0)}$ in (2.8a) obtained when the last term in that equation is replaced by $\mathcal{U}\vec{\mu}$; compare with (2.4). (Although $\vec{\mu}$ is not prescribed but instead is iteratively computed within the method, its exact value can still be used in the convergence analysis.) For Hamiltonian wave equations, \mathbf{L} is self-adjoint. Next, the conservation of \vec{Q} implies the orthogonality relation

$$\langle\mathcal{U}, \tilde{\mathbf{u}}_n\rangle = \vec{0}. \quad (2.11)$$

Taking the inner product between \mathcal{U} and (2.9a), one can show that Eq. (2.9b) does not change the linearization of (2.9a); the role of (2.9b) is to guarantee that the s components of vector \vec{Q} equal their prescribed values *exactly* rather than in the linear approximation. Thus, the operator in (2.10) is the linearized operator of the multi-component ITEM. Operator \mathcal{L} is easily verified [22] to be self-adjoint on the space of functions satisfying the orthogonality relation (2.11). However, $\mathbf{N}^{-1}\mathcal{L}$ is not self-adjoint. To cast the linearized ITEM (2.9) into a form involving only self-adjoint operators, which is more convenient to analyze than (2.10),

we use the following change of variables:

$$\tilde{\mathbf{v}}_n = \mathbf{N}^{1/2} \tilde{\mathbf{u}}_n, \quad \mathcal{V} = \mathbf{N}^{-1/2} \mathcal{U}, \quad \mathcal{K} = \mathbf{N}^{-1/2} \mathcal{L} \mathbf{N}^{-1/2}, \quad \mathbf{K} = \mathbf{N}^{-1/2} \mathbf{L} \mathbf{N}^{-1/2}. \quad (2.12)$$

Then the linearized ITEM (2.10) and the orthogonality relation (2.11) become:

$$\tilde{\mathbf{v}}_{n+1} - \tilde{\mathbf{v}}_n = \mathcal{K} \tilde{\mathbf{v}}_n \Delta\tau, \quad \mathcal{K} \tilde{\mathbf{v}}_n \equiv \mathbf{K} \tilde{\mathbf{v}}_n - \mathcal{V} \langle \mathcal{V}, \mathcal{V} \rangle^{-1} \langle \mathcal{V}, \mathbf{K} \tilde{\mathbf{v}}_n \rangle, \quad (2.13)$$

$$\langle \mathcal{V}, \tilde{\mathbf{v}}_n \rangle = \vec{0}. \quad (2.14)$$

In what follows we will analyze the transformed form (2.13) of the linearized ITEM, because it involves operator \mathcal{K} that is self-adjoint on the space of functions satisfying the orthogonality relation (2.14). Therefore, the evolution of the iteration error $\tilde{\mathbf{v}}_n$ is completely determined by the eigenvalues of \mathcal{K} . For convergence of the ITEM, these eigenvalues must lie between $-2/\Delta\tau$ and 0. The first of these conditions is achieved by adjusting $\Delta\tau$, whereas the second condition is analyzed in the next Section, where we will establish its connection to the number of positive eigenvalues of \mathbf{L} . It should be pointed out that by Sylvester's law of inertia (see, e.g., [9]), *the numbers of positive and zero eigenvalues of \mathbf{K} and \mathbf{L} are the same*. Therefore, we will refer everywhere to those eigenvalues of \mathbf{L} , whereas in the analysis of (2.13) it is the eigenvalues of \mathbf{K} that are involved directly.

Finally, a note is in order about the effect of zero eigenvalues of \mathbf{L} . As in [22], we assume the generic situation whereby the null space of \mathbf{L} does not contain any functions other than those of the modes $\partial \mathbf{u} / \partial x^{(k)}$ which are associated with translational invariance of the solitary wave along coordinate $x^{(k)}$. As was shown in [22] and [15] for the single-component ITEM and CGM, such modes lead only to a slight shift of the solitary wave along the respective coordinates, but do not otherwise affect convergence of the iterative method. The same proofs carry over directly to the multi-component case. Thus, in what follows we will focus on nonzero eigenvalues of \mathbf{L} .

3 Stability criterion for multi-component iterative methods

This Section contains the main result of this work, Eqs. (3.1), which are derived using a combination of analyses of Refs. [22] and [17]³. Namely, we will show that the operator \mathcal{K} is negative definite on the space of functions satisfying (2.14) provided that the Jacobian matrix

$$\frac{\partial \vec{Q}}{\partial \vec{\mu}} \equiv \frac{\partial(Q^{(1)}, \dots, Q^{(s)})}{\partial(\mu^{(1)}, \dots, \mu^{(s)})} \quad \text{is nonsingular} \quad (3.1a)$$

and that

$$p(\mathbf{L}) = p \left(\frac{\partial \vec{Q}}{\partial \vec{\mu}} \right), \quad (3.1b)$$

³While many pieces of the analysis of this section can be found in [17], we found it expedient to write a self-contained account of it. Indeed, it would take one some effort to relate the two quite different setting and notations of that paper and this work. Even more nontrivial effort is needed to deduce the main result, Eqs. (3.1), of this work from the main results summarized in Section II of [17].

where the notation p is defined in (1.11). Also, vectors \vec{Q} and $\vec{\mu}$ are defined at the beginning of Section 2, and operators \mathcal{K} and \mathbf{L} are defined in (2.12) and after (2.10), respectively. Conditions (3.1) generalize conditions (1.12) for the multi-component ITEM (2.9) and modified CGM (A.1). As explained at the end of Section 2, *under these conditions the ITEM can be guaranteed to converge* by choosing $\Delta\tau$ to be sufficiently small (in practice, $\Delta\tau = O(1)$ [22, 21]). The modified CGM is guaranteed to converge provided that (3.1) hold.

Let Ψ be an eigenfunction of \mathcal{K} and Φ be an eigenfunction of \mathbf{K} (defined in (2.12)):

$$\mathcal{K}\Psi = \Lambda\Psi, \quad \mathbf{K}\Phi = \lambda\Phi. \quad (3.2)$$

Taking the inner product of \mathcal{V} with the first equation in (3.2) and using the definition of \mathcal{K} , one sees that eigenfunctions Ψ with $\Lambda \neq 0$ satisfy the orthogonality relation (2.14). However, the eigenfunction Ψ with $\Lambda = 0$ does *not*, in general, satisfy that relation, as we will see later on. Let us now expand Ψ and \mathcal{V} over the set of Φ 's:

$$\begin{aligned} \Psi &= \sum_m a_m \Phi_m(\mathbf{x}) + \int_{\text{cont}} a(\lambda) \Phi(\lambda, \mathbf{x}) d\lambda, \\ \mathcal{V} &= \sum_m \Phi_m(\mathbf{x}) \vec{B}_m^T + \int_{\text{cont}} \Phi(\lambda, \mathbf{x}) \vec{B}^T(\lambda) d\lambda. \end{aligned} \quad (3.3)$$

Here the two terms in each expansion correspond to the contributions of the discrete and continuous spectra of \mathbf{K} , and a 's are scalars and \vec{B} 's are $s \times 1$ vectors:

$$\vec{B}_m = \langle \mathcal{V}, \Phi_m \rangle, \quad \vec{B}(\lambda) = \langle \mathcal{V}, \Phi(\lambda) \rangle. \quad (3.4)$$

Here and below we do not indicate the dependence of Φ and Ψ on \mathbf{x} since it is always implied. Let us also denote an $s \times 1$ vector

$$\vec{H} = \langle \mathcal{V}, \mathcal{V} \rangle^{-1} \langle \mathcal{V}, \mathbf{K}\Psi(\Lambda) \rangle. \quad (3.5)$$

From the (3.2), (3.3), (3.5) one finds:

$$a_m = \vec{B}_m^T \vec{H} / (\lambda_m - \Lambda), \quad a(\lambda) = \vec{B}^T(\lambda) \vec{H} / (\lambda - \Lambda). \quad (3.6)$$

Substitution of these equations into the orthogonality relation (2.14), which is to be satisfied by $\Psi(\Lambda)$ for $\Lambda \neq 0$, yields:

$$R\vec{H} = \vec{0}, \quad R(\Lambda) \equiv \sum_m \frac{\vec{B}_m \vec{B}_m^T}{\lambda_m - \Lambda} + \int_{\text{cont}} \frac{\vec{B}(\lambda) \vec{B}^T(\lambda)}{\lambda - \Lambda} d\lambda. \quad (3.7)$$

Before continuing, we need to point out one important feature of the eigenvalue problem for $\Psi(\Lambda)$, which can be restated as

$$\mathbf{K}\Psi - \Lambda\Psi = \mathcal{V}\vec{H}. \quad (3.8)$$

Namely, the vector \vec{H} in it is *arbitrary*, and, therefore, by specifying different \vec{H} 's one obtains different Ψ 's for a given Λ . To verify this, one only needs to substitute $\mathbf{K}\Psi$ from

(3.8) into (3.5). This observation about \vec{H} being arbitrary allows one to reformulate the problem $R(\Lambda)\vec{H} = \vec{0}$ as follows:

$$\textit{Analyze under what conditions matrix } R(\Lambda) \textit{ can be singular for } \Lambda > 0. \quad (3.9)$$

If we find that $R(\Lambda)$ can be singular only for $\Lambda < 0$, this would imply that \mathcal{K} is negative definite (modulo the remark made at the end of Section 2) and hence the multi-component ITEM and modified CGM would converge. Again, note that in arriving at formulation (3.9), we have relied on the arbitrariness of \vec{H} . Indeed, if \vec{H} had not been arbitrary but instead determined by $\Psi(\Lambda)$, then the first equation in (3.7) would not have been equivalent to (3.9), since even though $R(\Lambda)$ could have been singular, the particular \vec{H} might not have necessarily been its eigenvector.

To address question (3.9), we study the eigenvalue problem for the $s \times s$ real and symmetric matrix R :

$$R\vec{\varphi} = \gamma(\Lambda)\vec{\varphi}. \quad (3.10)$$

Its eigenvalues can be found from the Rayleigh quotient:

$$\gamma(\Lambda) = \vec{\varphi}^T R \vec{\varphi} / \vec{\varphi}^T \vec{\varphi}. \quad (3.11)$$

From (3.11), (3.7), (3.4) and the completeness of the set of Φ 's one has:

$$\gamma(\Lambda \rightarrow +\infty) = -\langle \mathcal{V}\vec{\varphi}, \mathcal{V}\vec{\varphi} \rangle / (\vec{\varphi}^T \vec{\varphi} \Lambda) \rightarrow -0. \quad (3.12)$$

Here we have used the fact that rank of \mathcal{V} is s , since \mathcal{V} is constructed from s independent components of \vec{Q} ; hence $\mathcal{V}\vec{\varphi} \neq \vec{0}$. Similarly, one verifies that all the eigenvalues of R satisfy

$$d\gamma/d\Lambda < 0 \quad \text{when} \quad \Lambda \neq \lambda_m. \quad (3.13)$$

As $\Lambda \rightarrow \lambda_m$, the matrix $(\lambda_m - \Lambda)R \rightarrow \vec{B}_m \vec{B}_m^T$. The latter is a rank-one matrix, and hence only one of its eigenvalues is nonzero. Therefore, at $\Lambda = \lambda_m$, at most (see below) one eigenvalue of R has a simple pole singularity and the other eigenvalues are continuous functions of Λ .

The facts stated in the previous paragraph allow one to specify when R can be singular (i.e., one of $\gamma(\Lambda) = 0$) for $\Lambda > 0$. We will do so for generic cases first and at the end will consider the missed special cases. One should consider three possibilities:

$$(i) \quad s = p(\mathbf{K}), \quad (ii) \quad s > p(\mathbf{K}), \quad (iii) \quad s < p(\mathbf{K}). \quad (3.14)$$

Qualitatively different situations for possibilities (i) and (ii) are exemplified by Fig. 1(a-d). From panels (a,c) in this Figure one can see that $\gamma = 0$ does *not* occur for $\Lambda > 0$ provided that $p(\mathbf{K}) = p(R(0))$. From Fig. 1(b,d) it also follows that if $p(\mathbf{K}) > p(R(0))$, then there is always a $\gamma = 0$ for some $\Lambda > 0$. By inspection, one can convince oneself that these statements are true is the general case (i.e., for any s and $p(\mathbf{K})$) for possibilities (i) and

(ii). One can also see that the situation where $p(\mathbf{K}) < p(R(0))$ cannot occur. Indeed, by (3.12), all $\gamma(\Lambda \rightarrow +\infty) < 0$, and they can become positive only at λ_m 's. Hence the number of positive eigenvalues of $R(0)$ cannot exceed the number of positive λ_m 's, which is $p(\mathbf{K})$. Finally, in regards to possibility (iii), one can easily see (Fig. 1(e)) that there should always be a $\gamma = 0$ for some $\Lambda > 0$. To summarize, R does not become singular for positive Λ only when $p(\mathbf{K}) = p(R(0))$.

Thus, to arrive at conditions (3.1), we need to relate $R(0)$ with $\partial\vec{Q}/\partial\vec{\mu}$. First, in analogy to the first equation in (3.7),

$$R(0)\vec{H} = \langle \mathcal{V}, \Psi(0) \rangle. \quad (3.15)$$

As we noted after Eq. (3.2), the right-hand side of (3.15) does not, in general, vanish. We will now find $\Psi(0)$. From the definition of \mathbf{K} ,

$$\mathbf{K}\Psi(0) = \mathcal{V}\vec{H}. \quad (3.16)$$

On the other hand, consider Eq. (2.8a) written for the transformed operator $\mathbf{K}^{(00)\mathbf{v}} \equiv \mathbf{N}^{-1/2}\mathbf{L}^{(00)}\mathbf{u}$ and note that the last term in that equation is $\mathcal{V}\vec{\mu}$ (see (2.8c)). Differentiation of this equation with respect to $\mu^{(k)}$ yields:

$$\mathbf{K}\frac{\partial\mathbf{v}}{\partial\mu^{(k)}} = \mathcal{V}\mathbf{e}^{(k)}, \quad k = 1, \dots, s, \quad (3.17a)$$

where $\mathbf{v} = \mathbf{N}^{1/2}\mathbf{u}$ and $\mathbf{e}^{(k)}$ is the $s \times 1$ vector whose k th entry is 1 and the other entries are zero. Combining Eqs. (3.17a) for all k yields

$$\mathbf{K}\frac{\partial\mathbf{v}}{\partial\vec{\mu}} = \mathcal{V}, \quad (3.17b)$$

where $\partial\mathbf{v}/\partial\vec{\mu}$ is an $S \times s$ matrix. Now, comparison of (3.16) and (3.17b) shows that

$$\Psi(0) = \partial\mathbf{v}/\partial\vec{\mu} + \sum_l g^{(l)} \partial\mathbf{v}/\partial x^{(l)}, \quad (3.18)$$

where $g^{(l)}$ are arbitrary constants, and we have used our assumption that the null space of \mathbf{L} (and hence of \mathbf{K}) can consist only of translational-invariance eigenmodes. All such eigenmodes are orthogonal to \mathcal{V} , as can be seen by considering their inner products with (3.17b). Then the substitution of (3.18) into (3.15) and recalling that $\mathcal{V} = \delta\vec{Q}/\delta\mathbf{v}$ (see (2.8b) and (2.12)) yields $R(0)\vec{H} = \partial\vec{Q}/\partial\vec{\mu}\vec{H}$. Given the arbitrariness of \vec{H} (see the text after (3.8)), this implies that

$$R(0) = \partial\vec{Q}/\partial\vec{\mu}. \quad (3.19)$$

This fact along with the summary sentence found before Eq. (3.15) entails condition (3.1b) in the generic case.

Let us now consider special cases that we have glossed over. First, suppose one of the terms in the discrete sum in (3.7) with a $\lambda_m > 0$ is a zero matrix. This can occur only when $\vec{B} = \vec{0}$. Then by the first equation in (3.4), the corresponding eigenfunction Φ_m of \mathbf{K}

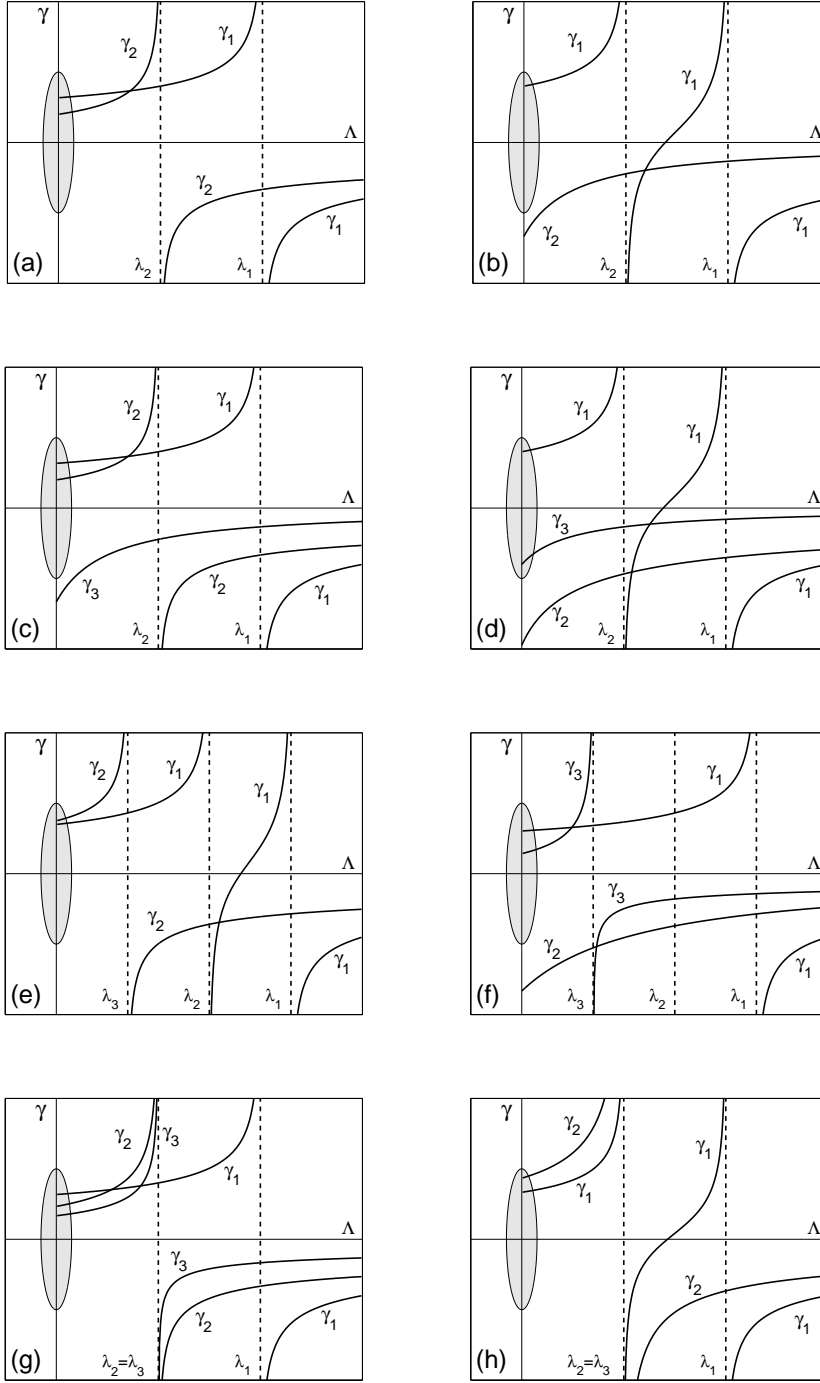


Figure 1: Various cases showing the eigenvalues of matrix $R(\Lambda)$, as explained in the text. The shaded oval along the vertical axis indicates that the curves which are depicted as crossing that axis at positive values can actually cross it anywhere (i.e., also at negative values). (a) $s = p(\mathbf{K}) = 2$; (b) $s = p(\mathbf{K}) = 2$; (c) $s = 3, p(\mathbf{K}) = 2$; (d) $s = 3, p(\mathbf{K}) = 2$; (e) $s = 2, p(\mathbf{K}) = 3$; (f) $s = p(\mathbf{K}) = 3$; (g) $s = p(\mathbf{K}) = 3$; (h) $s = 2, p(\mathbf{K}) = 3$.

satisfies the orthogonality condition (2.14) and, by (3.8) and (3.5), is also an eigenfunction of \mathcal{K} with the eigenvalue $\Lambda = \lambda_m > 0$. Thus, even though all the eigenvalues γ of $R(\lambda)$ are continuous at $\Lambda = \lambda_m$ and do not change their signs (see Fig. 1(f), where $\lambda_m = \lambda_2$), operator \mathcal{K} still has a positive eigenvalue $\Lambda = \lambda_m$. Note that since fewer than $p(\mathbf{K})$ of the eigenvalues γ change sign as Λ decreases from $+\infty$ to 0, then $p(R(0)) < p(\mathbf{K})$ and hence by (3.19), this special cases falls under the generic condition (3.1b).

Second, suppose that two positive eigenvalues of the self-adjoint operator \mathbf{K} are the same. Since the corresponding eigenfunctions are linearly independent, so are the eigenvectors of R whose eigenvalues will have a pole singularity at $\Lambda = \lambda_m$. Figures 1(g,h) illustrate two qualitatively different situations that can occur in this case. As one can see, condition (3.1b) still determines whether any of the $\gamma(\Lambda)$'s can vanish for $\Lambda > 0$.

Third, suppose $\partial\vec{Q}/\partial\vec{\mu} = R(0)$ is singular. This means that there is an eigenfunction $\Psi(0)$ of \mathcal{K} that satisfies the orthogonality condition (2.14). As we point out below, this may prevent the ITEM and modified CGM from converging. Hence we impose condition (3.1a). Thus, we have established both conditions (3.1) as being *sufficient* to guarantee that the iterative methods (2.9) (with (1.10) being satisfied) and (A.1) will converge for any initial guess \mathbf{u}_0 that is sufficiently close to the solitary wave being sought. \square

Let us now discuss how these methods may behave if either of these conditions is violated. If (3.1b) does not hold, then the ITEM is guaranteed to diverge for a generic initial condition, since the iteration error $\tilde{\mathbf{u}}_n$ will contain a component of the eigenmode that will increase by a factor $(1 + \Lambda\Delta\tau) > 1$ at each iteration. On the other hand, if (3.1a) is violated, then the iteration error will contain an eigenmode with $\Lambda = 0$, which will remain the same at each iteration. Hence the ITEM will settle near $(\mathbf{u} + \text{small constant} \cdot \Psi(0))$, and the norm of the iteration error will not be able to reach an arbitrarily low prescribed error. Thus, the linearized convergence analysis predicts that the method will “stall” at a higher error, but will not diverge. (Taking into account terms nonlinear in \tilde{u}_n (see (1.7)) may yield the information of whether the method actually converges or diverges. However, such a nonlinear analysis is of limited practical use since, even if the ITEM is found to eventually converge, it would do so very slowly in this case.)

As for the modified CGM, it is *not* bound to diverge if \mathcal{K} is not negative definite. However, it *may* do so when either of conditions (3.1) is violated. The mechanism of this divergence would be the vanishing of the denominator in Eqs. (A.1b,e) of the algorithm. Such a divergence can be avoided by choosing a different (but still generic) initial guess \mathbf{u}_0 .

Let us present an example where one can predict convergence of the ITEM and modified CGM without computing the eigenvalues of \mathbf{L} and $\partial\vec{Q}/\partial\vec{\mu}$. This example is a straightforward extension of Corollary 1 in [22] to the multi-component case. Consider a system of incoherently coupled NLS-type equations, generalizing (1.2):

$$iU_t^{(k)} + \nabla^2 U^{(k)} + G^{(k)}\left(|U^{(1)}|^2, \dots, |U^{(S)}|^2, \mathbf{x}\right) U^{(k)} = 0. \quad (3.20)$$

Its solitary wave is sought in the form $U^{(k)}(\mathbf{x}, t) = u^{(k)}(\mathbf{x}) \exp(i\mu^{(k)}t)$ with $u^{(k)}$ being real. Note that in this case, $s = S$, $\vec{Q} = (P^{(1)}, \dots, P^{(S)})$, and also

$$\mathbf{L} = \mathbf{L}^{(0)} + \mathcal{G}, \quad (\mathcal{G})^{(kl)} = 2u^{(k)}u^{(l)} \partial G^{(k)} / \partial (u^{(l)})^2. \quad (3.21a)$$

In this case the operator $\mathbf{L}^{(0)}$ is diagonal with entries

$$(\mathbf{L}^{(0)})^{(k)} = -\mu^{(k)} + \nabla^2 + G^{(k)}. \quad (3.21b)$$

Suppose that at least one of the components of \mathbf{u} has at least one node and \mathcal{G} is positive (semi)definite. Then $p(\mathbf{L}) > S$, and hence the iterative methods (2.9) and (A.1) diverge.

On the other hand, suppose that all components of \mathbf{u} are nodeless and \mathcal{G} is negative (semi)definite. Then $p(\mathbf{L}) = 0$, and hence the iterative methods converge. The proof of both statements repeats that of Corollary 1 in [22] and hence is not given here. \square

In general, when the number of quadratic conserved quantities is greater than 1 ($s > 1$), a geometric interpretation of the number $p(\partial\vec{Q}/\partial\vec{\mu})$ is rather obscure, in contrast to the interpretation of condition (1.12b). For completeness of presentation, we give a geometric interpretation of $p(\partial\vec{Q}/\partial\vec{\mu})$ for $s = 2$ in Appendix C.

4 Connection between convergence and dynamical stability

First, we observe that the conditions (3.1) under which the ITEM (2.9) and the modified CGM (A.1) are guaranteed to converge⁴ are the same under which the solitary wave of the incoherently coupled NLS-type equations (3.20) with all nodeless components is linearly stable [17]. (More precisely, the system analyzed in [17] had $G^{(k)} = \sum_{l=1}^S \sigma_{kl} |U^{(l)}|^2$, but the results of that paper are straightforwardly extended to apply to (3.20).) Thus, the nodeless solutions of (3.20) found by the iterative methods of this paper are guaranteed to be dynamically linearly stable. This is an extension of the result found in [22] for a single-component Eq. (1.2).

Let us now explain why this close connection between the convergence and stability takes place. Our explanation applies both to single- and multi-component equations. In regards to the convergence conditions, recall that the iteration methods converge when the operator \mathcal{L} in (2.10) is negative definite on the space of functions ψ satisfying the orthogonality relation (2.11). Note that on this space, $\langle \psi, \mathcal{L}\psi \rangle = \langle \psi, \mathbf{L}\psi \rangle$, and therefore, the negative definitenesses of \mathcal{L} and \mathbf{L} are equivalent under (2.11).

Let us now turn to the stability conditions. The details are slightly different for envelope and carrier solitary waves, so we begin with the former using Eqs. (2.1) as an example whenever needed. Seeking the slightly perturbed solitary wave in the form similar to (2.3)

⁴Recall that we always imply that (1.10) holds for the ITEM.

where now all $u^{(k)}$ are replaced by

$$u^{(k)} + (\tilde{u}_R^{(k)} + i\tilde{u}_I^{(k)})e^{\lambda t}, \quad u_{R,I}^{(k)}(\mathbf{x}) \in \mathbb{R}, \quad (4.1)$$

one obtains (see, e.g., [17]):

$$\mathbf{L}\tilde{\mathbf{u}}_R = \lambda\tilde{\mathbf{u}}_I, \quad \mathbf{L}_I\tilde{\mathbf{u}}_I = -\lambda\tilde{\mathbf{u}}_R. \quad (4.2)$$

In the case of Eqs. (2.3) or (3.20), $\mathbf{L}_I = \mathbf{L}^{(0)}$ (see (2.8a)), but in general (e.g., for the three-wave system [10, 5]) this is not so. Also, in the case where $s < S$, it is convenient, although not critical, to write the $\vec{\mu}$ -term in $\mathbf{L}_I\tilde{\mathbf{u}}_I$ as, e.g., for (2.4): $\text{diag}(\mu^{(1)}, \mu^{(2)}, \mu^{(1)}, \mu^{(2)})\tilde{\mathbf{u}}_I$; this makes \mathbf{L}_I explicitly self-adjoint. What is important is that

$$\mathbf{L}_I\mathcal{U} = \mathcal{O}, \quad (4.3)$$

where the right-hand side is the $S \times s$ zero matrix. Condition (4.3) is, in fact, the solvability condition of the second equation in (4.2), and is equivalent to the condition that $\tilde{\mathbf{u}}_R$ satisfy the orthogonality relation (2.11):

$$\langle \mathcal{U}, \tilde{\mathbf{u}}_R \rangle = \vec{0}. \quad (4.4)$$

Property (4.4) is easily verified by substituting (4.1) into the conservation law $d\vec{Q}/dt = \vec{0}$.

By (4.4), (4.3) one can invert the second equation in (4.2) and substitute the result in the first equation:

$$\mathbf{L}\tilde{\mathbf{u}}_R = -\lambda^2\mathbf{L}_I^{-1}\tilde{\mathbf{u}}_R. \quad (4.5)$$

Recall that this generalized eigenvalue problem is considered on the restricted space (4.4). Both operators in (4.5) are self-adjoint. Then, if \mathbf{L}_I^{-1} (and hence \mathbf{L}_I) is negative definite, then by Sylvester's law of inertia, the sign of λ^2 is determined by the signs of the eigenvalues of \mathbf{L} . If \mathbf{L} is negative definite (again — on the restricted space (4.4), or equivalently, (2.11)), then $\lambda^2 < 0$ and hence the solitary wave is dynamically linearly stable (see (4.1)).

Thus, to summarize: The conditions of convergence of the ITEM and modified CGM coincide with the conditions under which the solitary wave is dynamically linearly stable if and only if operator \mathbf{L}_I is negative definite. In particular, this occurs when \mathbf{u} is a ground state. (Unfortunately, the latter fact is not readily determined by inspection for multi-component solitary waves.) Let us note that this result about the coincidence of convergence and stability conditions for ground-state solitary waves fully agrees with the results of [2, 1], where it was proven that an ITEM-like method converges to ground states of (1.2) and its generalization (3.20) describing dynamics of Bose–Einstein condensates.

Finally, we give a counterpart of the above statement for carrier wave equations using the KdV equation

$$u_t + 2uu_x + u_{xxx} = 0 \quad (4.6)$$

as an example. Its solitary wave $u = u(x - ct) \equiv u(\xi)$ with velocity c satisfies an equation $u^2 - cu + u_{xx} = 0$, whose linearized operator is $L = 2u - c + \partial_x^2$. The iterative methods

seeking a solitary wave with a prescribed value of power (1.1) will converge provided that L is negative definite on a space of functions ψ satisfying a variant of (2.11):

$$\langle u, \psi \rangle = 0. \quad (4.7)$$

On the other hand, the stability analysis of (4.6) via an ansatz $u(x, t) = u(\xi) + \tilde{u}(\xi)e^{\lambda t}$ leads to the eigenvalue problem $\partial_x L \tilde{u} = \lambda \tilde{u}$. Upon the substitution $\tilde{w} = \partial_x^{-1} \tilde{u}$, this eigenvalue problem is rewritten in the same form as (4.2) [11]:

$$L\tilde{u} = \lambda\tilde{w}, \quad \mathbb{L}\tilde{w} = -\lambda\tilde{u}, \quad \mathbb{L} \equiv -\partial_x L \partial_x. \quad (4.8)$$

Note that due to the translational invariance of the solitary wave, u is a solution of $\mathbb{L}u = 0$. Thus, all considerations for the envelope equations carry over to the case of (4.6), and we conclude that the convergence conditions of the ITEM and CGM coincide with the stability conditions of the solitary wave if u is the ground state of \mathbb{L} (or, equivalently, \mathbb{L} is negative definite on the space defined by (4.7)).

It may also be pointed out that in coupled multi-component generalizations of the KdV, there is only one parameter — the wave's velocity c — that is the analog of the propagation constant vector $\vec{\mu}$ for the envelope equations, like in (2.1) or (3.20). Therefore, in this case, there is only one quadratic conserved quantity (which is probably the sum of the powers of all the components). In other words, $s = 1$, and hence the ITEM and modified CGM are guaranteed to converge only if $p(\mathbb{L}) \leq 1$.

5 Example: Ground state of spin-1 BEC in a magnetic field

Here we will demonstrate the validity of Eqs. (3.1) (more precisely, just Eq. (3.1b)), as the convergence condition of the ITEM (2.9). As an example, we use the equations of a spin-1 BEC, which have been actively studied in the last decade (see, e.g., references in [3, 16]). This example is slightly more complicated than that considered at the beginning of Section 2, in that its matrix $q^{(kl)}$, defined in (2.6), is not initially in REF (see (2.7)). Thus, by way of this example, we also illustrate how the normalization in (2.9b) (and also in (A.1c)) should be done when $q^{(kl)}$ is not initially in REF.

The time-dependent spin-1 BEC in a magnetic field can be described by the following set of nondimensional equations:

$$\begin{aligned} iU_t^{(1)} &= (\mathcal{C} + q + \beta_s(\rho^{(1)} + \rho^{(2)} - \rho^{(3)})) U^{(1)} + \beta_s(U^{(2)})^2 (U^{(3)})^*, \\ iU_t^{(2)} &= (\mathcal{C} + \beta_s(\rho^{(1)} + \rho^{(3)})) U^{(2)} + 2\beta_s U^{(1)} (U^{(2)})^* U^{(3)}, \\ iU_t^{(3)} &= (\mathcal{C} + q + \beta_s(\rho^{(2)} + \rho^{(3)} - \rho^{(1)})) U^{(3)} + \beta_s(U^{(1)})^* (U^{(3)})^2. \end{aligned} \quad (5.1a)$$

Here $U^{(1)}$, $U^{(2)}$, $U^{(3)}$ equal, respectively, ψ_1 , ψ_0 , ψ_{-1} in Eqs.(6)–(8) of [16]; $\rho^{(j)} = |U^{(j)}|^2$; and

$$\mathcal{C} = -\frac{1}{2}\partial_x^2 + \frac{1}{2}x^2 + \beta_n(\rho^{(1)} + \rho^{(2)} + \rho^{(3)}). \quad (5.1b)$$

The physical meaning of the coefficients q , β_s , β_n can be found in [16]. Note, in particular, that β_n in this section is *not* related to β_n in Appendices A and B. Note also that the coefficient p used in [16]⁵ is set to zero in (5.1) here without loss of generality: a nonzero p merely shifts the propagation constant $\mu^{(1)}$ defined in (5.3a) below.

Equations (5.1) have two quadraic conserved quantities:

$$Q_{\text{initial}}^{(1)} = \int (\rho^{(1)} - \rho^{(3)}) dx \quad \text{and} \quad Q_{\text{initial}}^{(2)} = \int (\rho^{(1)} + \rho^{(2)} + \rho^{(3)}) dx, \quad (5.2)$$

whose physical meaning can be found in [16, 3]. (The reason for the subscript ‘initial’ will become clear shortly.) Thus, in the notations introduced in Section 2, $S = 3$ and $s = 2$ for (5.1).

The stationary solution of (5.1) can be sought in the form

$$U^{(k)}(x, t) = u^{(k)}(x) \exp [i\mu^{(k)}t], \quad k = 1, 2, 3, \quad (5.3a)$$

where $u^{(k)}(x)$ can be taken real-valued [8], provided that

$$\mu^{(3)} = -\mu^{(1)} + 2\mu^{(2)}. \quad (5.3b)$$

Substitution of (5.3) into (5.2) yields:

$$\vec{Q}_{\text{initial}} = \begin{pmatrix} 1 & 0 & -1 \\ 1 & 1 & 1 \end{pmatrix} \begin{pmatrix} P^{(1)} \\ P^{(2)} \\ P^{(3)} \end{pmatrix}, \quad (5.4)$$

where $P^{(k)}$ are defined in (2.5). Note that the matrix in (5.4) is not in REF:

$$\text{REF of } \begin{pmatrix} 1 & 0 & -1 \\ 1 & 1 & 1 \end{pmatrix} = \begin{pmatrix} 1 & 0 & -1 \\ 0 & 1 & 2 \end{pmatrix}.$$

Accordingly, we redefine the vector of conserved quantities:

$$\vec{Q} = \begin{pmatrix} 1 & 0 & -1 \\ 0 & 1 & 2 \end{pmatrix} \begin{pmatrix} P^{(1)} \\ P^{(2)} \\ P^{(3)} \end{pmatrix} = \begin{pmatrix} P^{(1)} - P^{(3)} \\ P^{(2)} + 2P^{(3)} \end{pmatrix}. \quad (5.5)$$

Clearly, $Q^{(1)} = Q_{\text{initial}}^{(1)}$ and $Q^{(2)} = Q_{\text{initial}}^{(2)} - Q_{\text{initial}}^{(1)}$ are also quadratic conserved quantities of (5.1) (under reduction (5.3)).

Next, substitution of (5.3) into (5.1) yields a system

$$- \begin{pmatrix} (\mathcal{C} + q + \beta_s(\rho^{(1)} + \rho^{(2)} - \rho^{(3)})) u^{(1)} + \beta_s(u^{(2)})^2 u^{(3)} \\ (\mathcal{C} + \beta_s(\rho^{(1)} + \rho^{(3)})) u^{(2)} + 2\beta_s u^{(1)} u^{(2)} u^{(3)} \\ (\mathcal{C} + q + \beta_s(\rho^{(2)} + \rho^{(3)} - \rho^{(1)})) u^{(3)} + \beta_s u^{(1)} (u^{(2)})^2 \end{pmatrix} - \mathcal{U} \vec{\mu} = \mathbf{0}, \quad (5.6a)$$

⁵Again, no relation to $p(\mathbf{L})$ that has been used earlier in the present paper.

where, in accordance with (2.8) (see also (2.4)),

$$\mathcal{U} = \frac{\delta \vec{Q}}{\delta \mathbf{u}} = 2 \begin{pmatrix} u^{(1)} & 0 \\ 0 & u^{(2)} \\ -u^{(3)} & 2u^{(3)} \end{pmatrix}, \quad \vec{\mu} = \begin{pmatrix} \mu^{(1)} \\ \mu^{(2)} \end{pmatrix}. \quad (5.6b)$$

The first term in (5.6a) is what is denoted by $\mathbf{L}^{(00)}\mathbf{u}$ in (2.8a); the minus sign in front of it is dictated by the need to have a positive sign in front of ∂_x^2 : compare (5.6a) and (5.1b) with (2.4).

Implementation of method (2.9) for system (5.6) is then straightforward. The corresponding code can be found at

http://www.cems.uvm.edu/~lakobati/posted_papers_and_codes/2010_convergence. In particular, the normalization factors in (2.9b) become:

$$\sqrt{\left(Q^{(1)} - (-\hat{P}^{(3)})\right) / \hat{P}^{(1)}} \quad \text{for } k = 1, \quad (5.7a)$$

$$\sqrt{\left(Q^{(2)} - (2\hat{P}^{(3)})\right) / \hat{P}^{(2)}} \quad \text{for } k = 2. \quad (5.7b)$$

Note that the third component, $u^{(3)}$, is *not* normalized. This is the principal difference between our ITEM (2.9) and an ITEM proposed in [3, 16], whose authors had to use a fictitious normalization for $u^{(3)}$ in order to force both $Q^{(1)}$ and $Q^{(2)}$ to be preserved during the iterations. We believe that this difference makes our method simpler than the method of [3, 16], both in terms of implementation and conceptually.

To verify the validity of the convergence condition (3.1b), we have to independently compute, and then compare, both sides of that equation. To that end, we first found the solution of (5.6) by method (2.9) for the values of parameters similar to those used in [16]:

$$q = 0.1, \quad \beta_n = 240.8, \quad \beta_s = 7.5. \quad (5.8a)$$

The x -coordinate was chosen on the grid

$$x_l = -16 + (l - 1)\Delta x, \quad \Delta x = 1/8, \quad l = 1, \dots, 2^8. \quad (5.8b)$$

The acceleration operator \mathbf{N} in (2.9a) was chosen as

$$\mathbf{N} = \left(5 - \frac{1}{2}\partial_x^2\right) \begin{pmatrix} 1 & 0 \\ 0 & 1 \end{pmatrix},$$

and the parameter $\Delta\tau$ was set to 0.1 for $Q^{(2)} \geq 0.35$ and to 0.05 for $Q^{(2)} \leq 0.30$: a quick experimentation showed that these values resulted in reasonably fast convergence of the ITEM.

We varied $Q^{(1)}$ and $Q^{(2)}$ independently of each other in the range

$$Q_i^{(k)} = 0.10 + (i - 1) \cdot 0.05, \quad i = 1, 2, \dots, 21; \quad k = 1, 2. \quad (5.9)$$

The initial guess \mathbf{u}_0 was chosen for $Q_1^{(1)} = 0.10$, $Q_{21}^{(2)} = 1.10$ as

$$\begin{aligned} u^{(1)} &= 0.2 \exp \left[-\ln 2 (x/6)^2 \right], \\ u^{(2)} &= 0.3 \exp \left[-\ln 2 (x/4)^2 \right], \\ u^{(3)} &= -0.1 \exp \left[-\ln 2 (x/5)^2 \right]; \end{aligned} \quad (5.10)$$

this was motivated by Fig. 3a in [16]. Then, the initial guess for $Q_1^{(1)} = 0.10$, $Q_j^{(2)}$ with $j \leq 20$ was taken as the numerical solution for $Q_1^{(1)} = 0.10$, $Q_{j+1}^{(2)}$. For the pairs $Q_i^{(1)}$ with $i \geq 2$ and $Q_{21}^{(2)} = 1.10$, the initial guess was taken as the numerical solution for $Q_{i-1}^{(1)}$ and $Q_{21}^{(2)} = 1.10$; and then for a pair $Q_i^{(1)}$ with $i \geq 2$ and $Q_j^{(2)}$ with $j \leq 20$, the initial guess was taken as the solution for the “previous” pair, $Q_i^{(1)}$, $Q_{j+1}^{(2)}$. Shapes of solutions found in different parts of the region (5.9) are briefly described at the end of this section.

For each pair $(Q^{(1)}, Q^{(2)})$, the propagation constants were computed from (2.8c). Then, in order to compute the r.h.s. of (3.1b), we used the well-known fact that

$$\frac{\partial \vec{Q}}{\partial \vec{\mu}} = \left(\frac{\partial \vec{\mu}}{\partial \vec{Q}} \right)^{-1}. \quad (5.11)$$

The derivatives on the r.h.s. of (5.11) were obtained by the second-order accurate central-difference formula, e.g.:

$$\left. \frac{\partial \mu^{(2)}}{\partial Q^{(1)}} \right|_{ij} = \frac{\mu_{i+1,j}^{(2)} - \mu_{i-1,j}^{(2)}}{2 \cdot 0.05}, \quad i = 2, \dots, 20, \quad j = 1, \dots, 21; \quad (5.12a)$$

see (5.9). At the edges of the square defined by (5.9), we used a one-sided second-order accurate formulae, e.g.:

$$\left. \frac{\partial \mu^{(2)}}{\partial Q^{(1)}} \right|_{1j} = \frac{-\mu_{3,j}^{(2)} + 4\mu_{2,j}^{(2)} - 3\mu_{1,j}^{(2)}}{2 \cdot 0.05}, \quad j = 1, \dots, 21. \quad (5.12b)$$

The integer $p \left(\partial \vec{Q} / \partial \vec{\mu} \right)$ obtained in this way took on only values 0 and 1, as noted in Fig. 2.

To compute the l.h.s. of (3.1b), we first computed the linearization \mathbf{L} of (5.6); it is a self-adjoint operator, as mentioned after (2.10). We chose to arrange it so that it would act on the vector

$$\tilde{\mathbf{u}} \equiv (\tilde{\mathbf{u}}^{(1)}, \tilde{\mathbf{u}}^{(2)}, \tilde{\mathbf{u}}^{(3)})^T, \quad (5.13)$$

where each $\tilde{\mathbf{u}}^{(k)}$ was a vector taking on values on the grid (5.8b). Then the differential part, ∂_x^2 , of \mathbf{L} was approximated by the second-order formula, e.g.:

$$\partial_x^2 \tilde{u}_l^{(1)} \approx \left(\tilde{u}_{l+1}^{(1)} - 2\tilde{u}_l^{(1)} + \tilde{u}_{l-1}^{(1)} \right) / (\Delta x)^2, \quad l = 2, \dots, 255. \quad (5.14)$$

For simplicity, we chose zero Dirichlet boundary conditions for each $\tilde{\mathbf{u}}^{(k)}$; choosing a different type of boundary conditions (e.g., periodic) is expected to produce only a minor change to

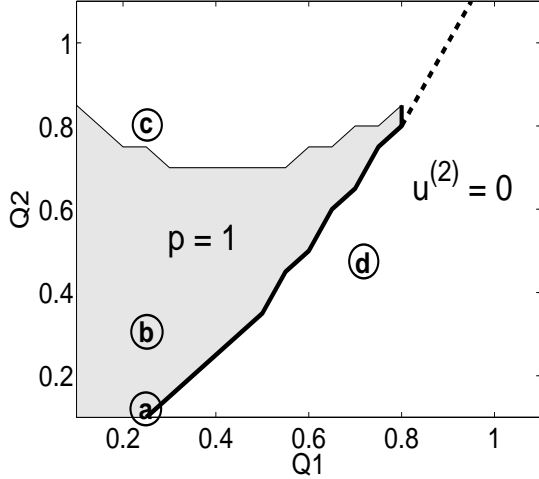


Figure 2: $p(\partial\vec{Q}/\partial\vec{\mu}) = p(\mathbf{L}) = 1$ in the shaded region and vanish everywhere else in this plot. See main text for further details. The circled letters a, b, c, d denote the “locations” of the solutions shown in Fig. 3.

the spectrum of \mathbf{L} . Thus, the discretized form of \mathbf{L} is a $3 \cdot 254 \times 3 \cdot 254$ real symmetric matrix, and its three largest eigenvalues were found with Matlab’s command `eigs(L,3,'LA')`.

Having compared $p(\partial\vec{Q}/\partial\vec{\mu})$ and $p(\mathbf{L})$ that were obtained as described above, we found that they coincided everywhere in the region (5.9) except at the curve plotted by the solid thick line in Fig. 2. At that curve, $p(\mathbf{L}) = 1$ and $p(\partial\vec{Q}/\partial\vec{\mu}) = 0$. This is really a minor discrepancy, since at that curve, the magnitude of the largest eigenvalue of \mathbf{L} is about 0.002, which is beyond the second-order accuracy of the approximation (5.14) on grid (5.8b). Also, the choice of the boundary conditions for \mathbf{L} , mentioned after (5.14), could contribute to that discrepancy. Thus, we conclude that the ITEM (2.9) converged to the solution of (5.6) when condition (3.1b) was satisfied. This supports the main result of this paper, which is that Eqs. (3.1) are sufficient conditions for convergence of the ITEM (2.9).

To conclude this section, in Fig. 3 we show a bi-product of our calculations: shapes of the ground-state solution of (5.6) in different parts of the region shown in Fig. 2. Let us note in passing that having $q \neq 0$ apparently has a profound effect on the solution’s shape. Indeed, it is straightforward (although tedious) to verify that for $q = 0$, Eqs. (5.6) possess a solution with all components being proportional to each other. Yet, when $q \neq 0$ (see (5.8a)), those components clearly lose that property. It may be interesting to obtain a solution of (5.6) with $q \ll 1$ from that with $q = 0$ by a perturbation theory; this, however, is not a subject of this work.

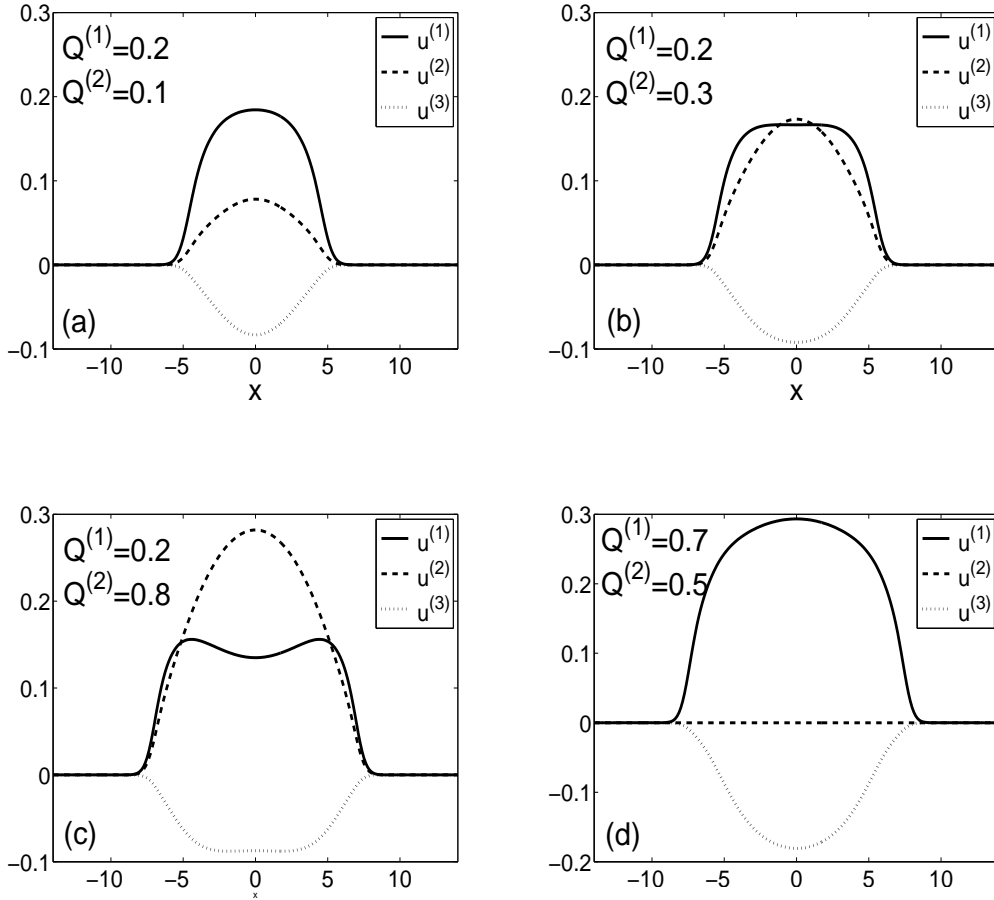


Figure 3: Typical shapes of solutions of (5.6), (5.8); the values of $Q^{(1,2)}$ are shown in the plots. Note that the solutions have a zero second component everywhere below the thick solid and dashed lines in Fig. 2. Above those lines, the solution for a fixed $Q^{(1)}$ follows the trend shown in panels (a)–(c) as $Q^{(2)}$ increases.

6 Conclusions

In this work, we obtained the convergence conditions of the iterative methods (2.9) and (A.1) that find multi-component solitary waves with prescribed values of quadratic conserved quantities (2.6). These convergence conditions are given by (3.1) (provided that (1.10) holds for the ITEM (2.9)), which extend the convergence conditions of the single-component ITEM obtained in [22]. These conditions also turn out to be the same as the dynamical stability conditions for the nodeless (e.g., ground-state) solitary wave of the system of incoherently coupled NLS-type equations (3.20), which were obtained in [17]. For a single-component NLS-type equation (1.2), such a coincidence was observed in [22]. Earlier, similar statements were proven for (1.2) and (3.20) in [1, 2] by different techniques. In Section 4 we showed that, in general, the convergence conditions of the iterative methods (2.9) and (A.1), on

one hand, and the dynamical stability conditions, on the other, coincide for ground-state solitary waves of all Hamiltonian nonlinear wave equations.

Let us conclude with two remarks. First, we reiterate that if the ITEM (2.9) converges slowly, then the modified CGM (A.1) will provide considerable acceleration of the iterations. Alternatively, one can use the slowest mode elimination technique [14] to accelerate the algorithm of the ITEM. Comparison of these three methods was done in [15], with the modified CGM being found the fastest.

Second, above we have explicitly mentioned the form of the operators employed by the ITEM and modified CGM for envelope equations (like (2.1) and (3.20)) and for the carrier waves (like the KdV, (4.6)). For systems that couple envelope and carrier waves, which are commonly referred to as short–long wave interaction, or generalized Zakharov–Benney, equations, the formalism remains the same.

Acknowledgement

I thank Dr. Y. Zhang for explaining to me the relation between the ITEM (2.9) of this paper and the methods proposed in [4, 3].

Appendix A: Modified CGM for solitary waves with a prescribed \vec{Q}

The steps of this algorithm for Eq. (2.8a) are very similar to those of the standard CGM (see, e.g., [19], Lecture 38), with the differences being in Eqs. (A.1c) and (A.1f) below. Recall that operator \mathcal{L} is defined in (2.10). Then the algorithm is:

$$\mathbf{r}_0 = \mathbf{N}^{-1}\mathbf{L}^{(0)}\mathbf{u}_0, \quad \mathbf{d}_0 = \mathbf{r}_0, \quad (\text{A.1a})$$

$$\alpha_n = -\frac{\langle \mathbf{N}\mathbf{d}_n, \mathbf{r}_n \rangle}{\langle \mathbf{d}_n, \mathcal{L}\mathbf{d}_n \rangle}, \quad (\text{A.1b})$$

$$\hat{\mathbf{u}}_{n+1} = \mathbf{u}_n + \alpha_n \mathbf{d}_n, \quad u_{n+1}^{(k)} = \hat{u}_{n+1}^{(k)} \sqrt{\frac{Q^{(k)} - \sum_{l=k+1}^S q^{(kl)} \hat{P}_{n+1}^{(l)}}{\hat{P}_{n+1}^{(k)}}}, \quad k = 1, \dots, s \leq S, \quad (\text{A.1c})$$

$$\mathbf{r}_{n+1} = \mathbf{N}^{-1}\mathbf{L}^{(0)}\mathbf{u}_{n+1} \quad (\text{A.1d})$$

$$\beta_n = -\frac{\langle \mathcal{L}\mathbf{d}_n, \mathbf{r}_{n+1} \rangle}{\langle \mathbf{d}_n, \mathcal{L}\mathbf{d}_n \rangle}, \quad (\text{A.1e})$$

$$\mathbf{d}_{n+1} = \mathbf{r}_{n+1} + \beta_n \mathbf{d}_n - \mathcal{U}_{n+1} \langle \mathcal{U}_{n+1}, \mathcal{U}_{n+1} \rangle^{-1} \langle \mathcal{U}_{n+1}, \beta_n \mathbf{d}_n \rangle. \quad (\text{A.1f})$$

Equation (A.1a) defines the initial residual \mathbf{r}_0 and the search direction \mathbf{d}_0 . The first equation in (A.1c) updates the iterative solution along the search direction \mathbf{d}_n by making a “step” of “length” α_n found in (A.1b). Equations (A.1d,f) update the residual and the

search direction using an auxiliary parameter β_n computed in (A.1e). Further justification of the steps of the algorithm is found in [15]. Note, however, that Eqs. (A.1a,e,f) have a simpler form than the corresponding equations, (5.20a,e,f), in [15], because in the present paper we realized that

$$\langle \mathcal{U}_n, \mathbf{r}_n \rangle = 0 \quad (\text{A.2})$$

for all n (see (A.1d) and (2.8a)). Then, Eqs. (A.1a,f) and (A.2) guarantee that $\langle \mathcal{U}_n, \mathbf{d}_n \rangle = 0$ for all n also.

Appendix B: Forms of algorithms (2.9) and (A.1) for complex-valued equations

Here we show how algorithms (2.9) and (A.1) can be applied to complex-valued equations directly, i.e. without splitting them into real and imaginary parts.

In fact, the equations of the ITEM (2.9) do not change, and the only difference from the real-valued case is that now

$$\mathcal{U} = \frac{\delta \vec{Q}}{\delta \mathbf{u}^*} \quad (\text{B.1})$$

and that the inner product must be defined as

$$\langle f(\mathbf{x}), g(\mathbf{x}) \rangle \equiv \int (f(\mathbf{x}))^\dagger g(\mathbf{x}) d\mathbf{x}, \quad (\text{B.2})$$

where \dagger denotes Hermitian conjugation. Also, $\mathbf{L}^{(0)}\mathbf{u}_n$ is now a complex-valued vector.

In addition to these minor changes, the CGM (A.1) required a few other modifications. We will first explain the idea of how those modifications can be arrived at, and then will state the modified form of (A.1). First, note that operator \mathbf{L} , defined after (2.10), should be modified as follows:

$$\mathbf{L}^{(0)}(\mathbf{u} + \tilde{\mathbf{u}}) = \frac{\delta (\mathbf{L}^{(0)}\mathbf{u})}{\delta \mathbf{u}} \tilde{\mathbf{u}} + \frac{\delta (\mathbf{L}^{(0)}\mathbf{u})}{\delta \mathbf{u}^*} \tilde{\mathbf{u}}^* \equiv \mathbf{L}_{\text{self}}\tilde{\mathbf{u}} + \mathbf{L}_{\text{conj}}\tilde{\mathbf{u}}^*. \quad (\text{B.3a})$$

Here, as before, \mathbf{u} is the exact solution of (2.8a) and $\tilde{\mathbf{u}}$ is a small deviation from it. For example, if $L^{(0)}u = u_{xx} + u|u|^2 - \mu u$, then $L_{\text{self}} = (-\mu + \partial_x^2) + 2|u|^2$ and $L_{\text{conj}} = u^2$. Thus, while $\mathbf{L}^{(0)}$ acts on an S -component vector \mathbf{u} , \mathbf{L} must act on a $2S$ -component vector $(\tilde{\mathbf{u}}, \tilde{\mathbf{u}}^*)^T$:

$$\mathbf{L} \begin{pmatrix} \tilde{\mathbf{u}} \\ \tilde{\mathbf{u}}^* \end{pmatrix} = \begin{pmatrix} \mathbf{L}_{\text{self}} & \mathbf{L}_{\text{conj}} \\ \mathbf{L}_{\text{conj}}^* & \mathbf{L}_{\text{self}}^* \end{pmatrix} \begin{pmatrix} \tilde{\mathbf{u}} \\ \tilde{\mathbf{u}}^* \end{pmatrix}. \quad (\text{B.3b})$$

Then, as an auxiliary step towards the generalization of (A.1) to complex-valued functions, one replaces vectors and matrices there by their “extended” versions, e.g.:

$$\mathbf{r}_n \rightarrow \begin{pmatrix} \mathbf{r}_n \\ \mathbf{r}_n^* \end{pmatrix}, \quad \mathcal{U}_n \rightarrow \begin{pmatrix} \mathcal{U}_n \\ \mathcal{U}_n^* \end{pmatrix}, \quad \text{etc.} \quad (\text{B.4})$$

Proceeding in this way, one obtains after straightforward algebra that algorithm (A.1) can be restated *for the original rather than “extended”, as in (B.4) quantities*⁶ as follows. Steps (a, c, d, f) of the modified algorithm are the same as the respective steps of (A.1), except that in (2.8a) and (A.1f), the terms $\langle \mathbf{N}^{-1}\mathcal{U}, \mathbf{L}^{(00)}\mathbf{u} \rangle$ and $\langle \mathcal{U}_{n+1}, \mathbf{d}_n \rangle$ are to be replaced by their respective real parts. Steps (b) and (e) of (A.1) change as follows:

$$\alpha_n = -\frac{\operatorname{Re}\langle \mathbf{N}\mathbf{d}_n, \mathbf{r}_n \rangle}{\operatorname{Re}\langle \mathbf{d}_n, \mathcal{L}_{\text{self}}\mathbf{d}_n + \mathcal{L}_{\text{conj}}\mathbf{d}_n^* \rangle}, \quad (\text{B.5b})$$

$$\beta_n = -\frac{\operatorname{Re}\langle \mathbf{r}_{n+1}, \mathcal{L}_{\text{self}}\mathbf{d}_n + \mathcal{L}_{\text{conj}}\mathbf{d}_n^* \rangle}{\operatorname{Re}\langle \mathbf{d}_n, \mathcal{L}_{\text{self}}\mathbf{d}_n + \mathcal{L}_{\text{conj}}\mathbf{d}_n^* \rangle}, \quad (\text{B.5e})$$

where (see (2.10) and (B.3))

$$\mathcal{L}_{\text{type}}\psi = \mathbf{L}_{\text{type}}\psi - \mathcal{U}\langle \mathbf{N}^{-1}\mathcal{U}, \mathcal{U} \rangle^{-1} \operatorname{Re}\langle \mathbf{N}^{-1}\mathcal{U}, \mathbf{L}_{\text{type}}\psi \rangle, \quad \text{‘type’} = \text{‘self’ or ‘conj’}.$$

Appendix C: Geometric interpretation of $p(\partial\vec{Q}/\partial\vec{\mu})$ when $s = 2$

In the case of a single equation, the ITEM’s convergence condition $\partial P/\partial\mu > 0$ in (1.12b) has a simple geometric interpretation: the curve $P(\mu)$ must have a positive slope. (In other words, solitary waves for which $p(L) = 1$ and curve $P(\mu)$ has a negative slope cannot be obtained by the ITEM; however, they may be obtained by other iterative methods [22].) The convergence condition in the multi-component case, Eq. (3.1b), is not as straightforward to visualize. Here we will give a geometric interpretation of this condition for the case $s = 2$, i.e. when the solitary wave has two quadratic conserved quantities $Q^{(1)}$ and $Q^{(2)}$. (Note that the solitary wave in this case can have more than two components: examples include the three-wave system [10, 5], Eqs. (2.1), and the spinor BEC equations considered in Section 5.) While in the $s = 1$ case the Jacobian $\partial\vec{Q}/\partial\vec{\mu} \equiv \partial P/\partial\mu$ can be either positive or nonpositive (i.e., there are *two* possibilities), in the $s = 2$ there are *three* possibilities: when $\partial\vec{Q}/\partial\vec{\mu}$ has two, one, or no positive eigenvalues. Thus, below we will give a geometric interpretation of these three situations. Interestingly, this interpretation makes reference of a single curve (see Eqs. (C.5) below) — an intersection line of surfaces $Q^{(1)}(\mu^{(1)}, \mu^{(2)})$ and $Q^{(2)}(\mu^{(1)}, \mu^{(2)})$ shifted in a certain manner.

For brevity, let us denote

$$\frac{\partial\vec{Q}}{\partial\vec{\mu}} \equiv \begin{pmatrix} \partial Q^{(1)}/\partial\mu^{(1)} & \partial Q^{(2)}/\partial\mu^{(1)} \\ \partial Q^{(1)}/\partial\mu^{(2)} & \partial Q^{(2)}/\partial\mu^{(2)} \end{pmatrix} = \begin{pmatrix} a_{11} & a_{12} \\ a_{12} & a_{22} \end{pmatrix}. \quad (\text{C.1})$$

Note that $\partial\vec{Q}/\partial\vec{\mu} = R(0)$ is a symmetric matrix (see (3.7)), and so $a_{21} = a_{12}$. From the quadratic equation satisfied by its eigenvalues one can see that:

$$\det(\partial\vec{Q}/\partial\vec{\mu}) > 0 \text{ and } a_{11}, a_{22} > 0 \quad \Rightarrow \quad p(\partial\vec{Q}/\partial\vec{\mu}) = 2; \quad (\text{C.2a})$$

⁶I.e., \mathbf{r}_n , \mathbf{d}_n , and \mathbf{u}_n are S -component and *not* $2S$ -component vectors, and \mathcal{U} is an $S \times s$ matrix.

$$\det(\partial\vec{Q}/\partial\vec{\mu}) < 0 \quad \Rightarrow \quad p(\partial\vec{Q}/\partial\vec{\mu}) = 1; \quad (\text{C.2b})$$

$$\det(\partial\vec{Q}/\partial\vec{\mu}) > 0 \text{ and } a_{11}, a_{22} < 0 \quad \Rightarrow \quad p(\partial\vec{Q}/\partial\vec{\mu}) = 0. \quad (\text{C.2c})$$

We have used the symmetry of $\partial\vec{Q}/\partial\vec{\mu}$ to infer that a definite sign of $(a_{11} + a_{22})$ in (C.2a,c) implies the corresponding sign for *both* these diagonal entries individually.

Let us consider two surfaces $Q^{(1)}(\mu^{(1)}, \mu^{(2)})$ and $Q^{(2)}(\mu^{(1)}, \mu^{(2)})$ and the normal vectors to them at a given point $(\mu^{(1)}, \mu^{(2)})$:

$$\underline{n}_k = [a_{k1}, a_{k2}, -1], \quad k = 1, 2, \quad (\text{C.3})$$

where these vectors are chosen to point downward. If these surfaces are vertically shifted so as to have the same height at point $(\mu^{(1)}, \mu^{(2)})$, then the cross-product of the normal vectors defines the direction of the intersection line of such shifted surfaces at this point. The vertical component of this cross-product is $\det(\partial\vec{Q}/\partial\vec{\mu})$:

$$\underline{n}_1 \times \underline{n}_2 = \begin{vmatrix} \underline{i} & \underline{j} & \underline{k} \\ a_{11} & a_{12} & -1 \\ a_{21} & a_{22} & -1 \end{vmatrix}. \quad (\text{C.4})$$

Thus, according to the above definition, the intersection line, ℓ , of the shifted surfaces $Q^{(1)}(\mu^{(1)}, \mu^{(2)})$ and $Q^{(2)}(\mu^{(1)}, \mu^{(2)})$ points in the same vertical direction (i.e., up or down) as $\underline{n}_1 \times \underline{n}_2$. Let us also note that (a_{k1}, a_{k2}) are the projections of \underline{n}_k onto the axes $\mu^{(1)}$ and $\mu^{(2)}$. With these observations, conditions (C.2) are restated as:

$$\begin{array}{l} \ell \text{ points up and} \\ \text{projection of } \underline{n}_k \text{ on respective axis } \mu^{(k)} \text{ is } \textit{positive} \end{array} \quad \Rightarrow \quad p(\partial\vec{Q}/\partial\vec{\mu}) = 2; \quad (\text{C.5a})$$

$$\ell \text{ points down} \quad \Rightarrow \quad p(\partial\vec{Q}/\partial\vec{\mu}) = 1; \quad (\text{C.5b})$$

$$\begin{array}{l} \ell \text{ points up and} \\ \text{projection of } \underline{n}_k \text{ on respective axis } \mu^{(k)} \text{ is } \textit{negative} \end{array} \quad \Rightarrow \quad p(\partial\vec{Q}/\partial\vec{\mu}) = 0. \quad (\text{C.5c})$$

Finally, let us note that conditions (C.5) can be restated solely in terms of the two-component vectors $\vec{a}_k \equiv [a_{k1}, a_{k2}]$ obtained by projection of \underline{n}_k on the horizontal plane:

$$\begin{array}{l} \text{angle between } \vec{a}_1 \text{ and } \vec{a}_2 \text{ is } < 180^\circ \text{ and} \\ \text{projection of } \vec{a}_k \text{ on respective axis } \mu^{(k)} \text{ is } \textit{positive} \end{array} \quad \Rightarrow \quad p(\partial\vec{Q}/\partial\vec{\mu}) = 2; \quad (\text{C.6a})$$

$$\text{angle between } \vec{a}_1 \text{ and } \vec{a}_2 \text{ is } > 180^\circ \quad \Rightarrow \quad p(\partial\vec{Q}/\partial\vec{\mu}) = 1; \quad (\text{C.6b})$$

$$\begin{array}{l} \text{angle between } \vec{a}_1 \text{ and } \vec{a}_2 \text{ is } < 180^\circ \text{ and} \\ \text{projection of } \vec{a}_k \text{ on respective axis } \mu^{(k)} \text{ is } \textit{negative} \end{array} \quad \Rightarrow \quad p(\partial\vec{Q}/\partial\vec{\mu}) = 0, \quad (\text{C.6c})$$

where the angle is measured from \vec{a}_1 to \vec{a}_2 in the counterclockwise direction.

References

- [1] W. Bao, Ground states and dynamics of multi-component Bose-Einstein condensates, *Multiscale Model. Simul.* 2 (2004) 210–236.
- [2] W. Bao, Q. Du, Computing the ground state solution of Bose–Einstein condensates by a normalized gradient flow, *SIAM J. Sci. Comput.* 25 (2004) 1674–1697.
- [3] W. Bao, F.Y. Lim, Computing ground states of spin-1 Bose–Einstein condensates by the normalized gradient flow, *SIAM J. Sci. Comput.* 30 (2008) 1925–1948.
- [4] W. Bao, H. Wang, A mass and magnetization conservative and energy-diminishing numerical method for computing ground state of spin-1 Bose–Einstein condensates, *SIAM J. Numer. Anal.* 45 (2007) 2177–2200.
- [5] A.V. Buryak, P. Di Trapani, D.V. Skryabin, S. Trillo, Optical solitons due to quadratic nonlinearities: From basic physics to futuristic applications, *Phys. Rep.* 370 (2002) 63–235.
- [6] M.L. Chiofalo, S. Succi, M.P. Tosi, Ground state of trapped interacting Bose-Einstein condensates by an explicit imaginary-time algorithm, *Phys. Rev. E* 62 (2000) 7438–7444.
- [7] J.J. Garcia-Ripoll, V.M. Perez-Garcia, Optimizing Schrödinger functionals using Sobolev gradients: Applications to Quantum Mechanics and Nonlinear Optics, *SIAM J. Sci. Comput.* 23 (2001) 1316–1334.
- [8] T. Isoshima, K. Machida, T. Ohmi, Spin-domain formation in spinor Bose–Einstein condensation, *Phys. Rev. A* 60 (1999) 4857–4863.
- [9] R. Horn, C. Johnson, *Matrix Analysis*, Cambridge University Press, Cambridge, 1991 [specifically, see Theorems 4.5.8 and 7.6.3].
- [10] Y. N. Karamzin, A. P. Sukhorukov, Mutual focusing of high-power light beams in media with quadratic nonlinearity, *Sov. Phys. JETP* 41 (1976) 414–420.
- [11] Y. Kodama, D. Pelinovsky, Spectral stability and time evolution of N-solitons in the KdV hierarchy, *J. Phys. A: Math. Gen.* 38 (2005) 6129–6140.
- [12] A.A. Kolokolov, Stability of stationary solutions of nonlinear wave equations, *Radio-phys. Quantum Electron.* 17 (1974) 1016–1020.
- [13] T.I. Lakoba, D.J. Kaup, B.A. Malomed, Solitons in nonlinear directional coupler with two orthogonal polarizations, *Phys. Rev. E* 55 (1997) 6107–6120.

- [14] T.I. Lakoba, J. Yang, A mode elimination technique to improve convergence of iteration methods for finding solitary waves, *J. Comp. Phys.* 226 (2007) 1693–1709.
- [15] T.I. Lakoba, Conjugate gradient method for finding fundamental solitary waves, *Physica D* 238 (2009) 2308–2330.
- [16] F.Y. Lim, W. Bao, Numerical methods for computing the ground state of spin-1 Bose–Einstein condensates in a uniform magnetic field, *Phys. Rev. E* 78 (2008) 066704.
- [17] D.E. Pelinovsky, Y.S. Kivshar, Stability criterion for multicomponent solitary waves, *Phys. Rev. E* 62 (2000) 8668–8676.
- [18] V.S. Shchesnovich, S.B. Cavalcanti, Rayleigh functional for nonlinear systems, available at <http://www.arXiv.org>, Preprint nlin.PS/0411033.
- [19] L.N. Trefethen, D. Bau, III, *Numerical Linear Algebra*, SIAM, Philadelphia, 1997.
- [20] N.G. Vakhitov, A.A. Kolokolov, Stationary solutions of the wave equation in the medium with nonlinearity saturation, *Radiophys. Quantum Electron.* 16 (1973) 783–789.
- [21] J. Yang, T.I. Lakoba, Universally-convergent squared-operator iteration methods for solitary waves in general nonlinear wave equations, *Stud. Appl. Math.* 118 (2007) 153–197.
- [22] J. Yang, T.I. Lakoba, Accelerated imaginary-time evolution methods for the computation of solitary waves, *Stud. Appl. Math.* 120 (2008) 265–292.